Dynamic Mechanical Properties of Human Skin

K. Kong[1], M. DeWitt[2], M. Danilich[2], B. Gillich[3], **M. B. Panzer**[1]

[1]*University of Virginia, 4040 Lewis and Clark Dr. Charlottesville, 22911 VA., USA*
panzer@virginia.edu
[2]*Luna Innovations, 706 Forest St., Charlottesville, 22901 VA., USA,*
[3]*U.S. Army Aberdeen Test Center, 6943 Colleran Rd B400, APG, 21005-5059 MD., USA*

Abstract. Skin is the largest human organ which has many functions, including the initial protection of the human body from injury. Therefore, understanding of mechanical properties of the skin is crucial for various applications, including non-lethal ballistics development where the goal is effective deterrence while avoiding penetrating or irreversible damaging of the skin during impact. The objective of this study is to quantify the tensile mechanical properties and failure response of human skin through dynamic tests. A total of 108 skin samples were obtained from the posterior torsos of six post-mortem human subjects for experimental testing. The skin samples were tested in comprehensive battery of tests, including quasi-static and dynamic tension (uniaxial) to failure, tensile stress relaxation (uniaxial), compression, and dynamic indentation (biaxial) to failure. The skin samples were marked in the *in-situ* reference state before removal. On one side of the torso, dog-bone test samples for uniaxial tension tests were prepared by orienting the axis of loading at 0° and 90° respectively with respect to identified Langer lines. On the other side, square patches (approximately 75 x 75 mm) were prepared for the dynamic indentation tests. All samples were stored in a dampened environment of saline to prevent moisture loss. During the testing, all samples were preloaded to match the *in situ* stretch state before any mechanical loading. Destructive tensile tests, compression tests, and stress relaxation tests of human skin were performed across different strain-rates (up to 180 1/s) and *in situ* orientations. The results of this study will be used for informing the development of constitutive models of skin for human body modeling, and skin simulants used in the physical test and evaluation environment for assessing the safety of protective body armor and/or blunt non-lethal weapons.

1. INTRODUCTION

Human skin is a delicate organ that can easily result in injury when subjected to loading conditions such as scraping, tearing, and penetrating. Open skin wounds can potentially allow severe blood loss and lead to infection or chronic conditions, which affects 4.5 million people in the United States [1]. Understanding the biomechanics of the skin, and its threshold for failure, is vital for improving the efficacy of safety equipment and protective gear in preventing skin injury in many applications including transportation safety, law enforcement, and in the military. Knowing the biomechanics of skin is equally important to the development of non-lethal blunt projectiles, which are not intended to cause penetration.

To study skin injury mechanics, animal skin tissue collected from mice and goats have been studied but were found to not represent the human skin respectively in terms of ultimate stress [2,3]. Porcine skins have been reported to be like the human skin when looking at elastic modulus and ultimate stress but was found to rupture at lower strain levels [4]. Chamois skin was also used as part of skin surrogate's development for skin penetration assessment showed acceptable biofidelic results, however, its thickness inconsistency and reproducibility reduce its practicality [5,6]. Efforts have been made to develop affordable synthetic skin simulant (silicone and urethane) with a stable shelf life to exhibit biomechanical failure equivalence to human skin also show little success [7].

Skin is reported to be non-linear, anisotropic, and viscoelastic [8]. Generally, skin shows stiffer response when loaded along its collagen fiber direction than across fiber direction under tension. The fiber recruitment contributes to the anisotropic behavior and therefore provides full strength of the skin when loaded under tension compared to compression and shear. Skin rupture data is necessary to study open skin injuries and therefore in-vitro skin testing is desired compared to in-vivo skin testing. Several destructive tensile tests of in-vitro human skin have been conducted in the past [9-11] looking into either the effect of loading rate or skin orientation with respect to Langer line on skin tensile failure behavior. To date, Ottenio et al. (2015) have provided a first comprehensive dataset regarding mechanical failure properties of human skin by considering anisotropy, strain rate effect (0.06/s-167/s) and skin failure simultaneously despite only one post-mortem human subject (PMHS) was studied [12]. The lack of having inter-subject variation simplifies investigation on the strain rate and orientation effect on skin behavior but this also limits the practicality of the skin data for representing the human population. In addition, neither of these tests provides viscoelastic data of the human skin although it has been shown the human skin response is strain rate dependent [12]. The collection of viscoelastic data is deemed

https://doi.org/10.52202/078352-0031

necessary for skin constitutive model development. Viscoelastic tests of human skin were conducted in-vivo where small stretch/stress levels were applied to living human subjects through suction [13,14]. However, these in-vivo studies do not allow viscoelastic information at high stretch levels to be determined and effects from surrounding tissues cannot be eliminated.

This study provides new viscoelastic and destructive tensile stress-stretch response of human skin by considering inter-subject variation with strain rate applicable in between automotive crash and ballistic impact event in the field of injury biomechanics. The in-vitro viscoelastic dataset is expected to inform the selection of an appropriate constitutive model that can be used to model human skin tensile response. The destructive tensile test series will provide a relationship between strain rate and sub-failure initiation for different skin orientations. Identification of the sub-failure initiation will also help to bound the stress-stretch region that contains the skin undamaged response in which the pristine constitutive model can be applied to. Ultimately, this data will be used to develop constitutive models of skin for use in simulating blunt impact events with human body models.

2. METHODS

Skin samples were excised from the back of six male PMHS at the Center for Applied Biomechanics, University of Virginia (UVA), USA. All test procedures were approved by the UVA Institutional Review Board prior to any testing and the PMHS were screened for pre-existing pathologies to avoid skin diseases that may affect skin quality. The PMHS represent an average of 57±11 years old, 178.6±3.8 cm in height and weighed 88.4±19.8 kg adult male (Table 1).

Table 1. Post-mortem human subject information

Specimen ID	Age (years)	Height (cm)	Weight(kg)
795	60	175.3	83.9
757	49	185.4	122
702	42	178	86
733	74	180.3	78.9
919	59	177.8	96.6
680	58	175	63

2.1 Sample Preparation

All the PMHS were thawed for three days in a room temperature environment before skin excision took place. The orientation of the skin sample is determined with reference to anatomy illustration of Langer line [15], and both parallel (0°) and perpendicular (90°) samples with respect to the Langer line were included for testing (Figure 1, left). Custom printed stencils and sharpie markers were used to mark the contour and in-vivo dimension of the skin samples prior to excision (Figure 1, center). After marking, a surgical scalpel was used to excise the skin samples and excessive adipose tissues were carefully scraped off (Figure 1, right). This completes the skin excision process and each skin sample was wrapped in saline dampened gauze pad to prevent moisture loss and refrigerated at 4°C until testing which was within 48 hours. For each PMHS, two different sizes of skin samples were excised on the left side of the back for uniaxial tensile (static and dynamic) and stress relaxation tests, the contralateral side of the back was reserved for other skin samples for a different study. An additional cutting step was performed during the day of testing where the skin was cut into a dogbone shape using a custom made hardened steel cutter based on ASTM D412 standard test method for the dynamic tensile (DT) test while a scaled version of the standard was used to cut the dogbone skin samples for the static tensile (ST) and stress relaxation (SR) test. The purpose is to maximize the numbers of skin sample within individual PMHS specimen for different test series and a total of 72 (48 tensile test samples and 24 stress relaxation test samples) skin samples were collected from the six PMHS. Each skin sample thickness was measured using a digital caliper prior to testing and the measured mean thickness was 3.33±0.87 mm.

https://doi.org/10.52202/078352-0031

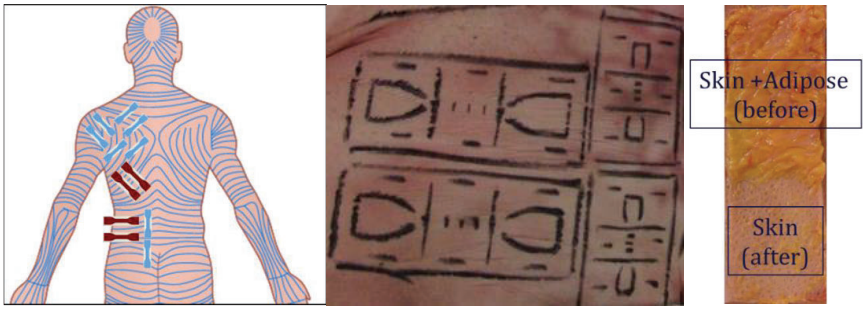

Figure 1. (left) Locations of skin samples on the left side of the human back (blue – static tensile samples (n=4) and stress relaxation samples (n=4), red – dynamic tensile test samples (n=4)). (center) Marked in-vivo state of human skin before excision. (right) Skin samples with underlying adipose (before) versus isolated skin samples without adipose (after).

2.2 Uniaxial Tensile Tests

The ST tests were performed using the Instron Model 8874 servohydraulic actuated test machine (Instron, Canton, MA) and a custom-built gravity-based drop tower was used for the DT tests (Figure 2). Dogbone sample was clamped with additional 80 grit sandpapers at both ends of the test fixture to avoid slippage during testing. After clamping, the skin sample was loaded until reaching its in-vivo length by comparing to an in-vivo reference length rod (Figure 4) before initiating the test. The test was initiated by moving the crosshead of the machine until skin failure occurred. Both parallel and perpendicular samples were tested at static (1/s) and dynamic (75/s and 180/s) engineering strain-rates, similar strain-rate levels conducted by Ottenio et al. (2015). A 1000 lbf (4.4 kN) Honeywell model 31 piezoresistive load cell (Honeywell, Charlotte, NC) was used to measure the force at 1000 and 10,000 sampling rates for ST and DT tests, respectively. Similarly, videos were recorded at 1000 fps for ST tests and 10,000 fps for DT tests using a Memrecam GX-1 high-speed camera (NAC Image Technology, Simi Valley, CA). Sharpie markers which were predetermined on the PMHS before skin excision were used for determining stretch values through video tracking software (Figure 3) (Tracker, ver. 4.11.0). A trigger box was utilized to activate data acquisition of the load cell and video recording simultaneously when the test was initiated.

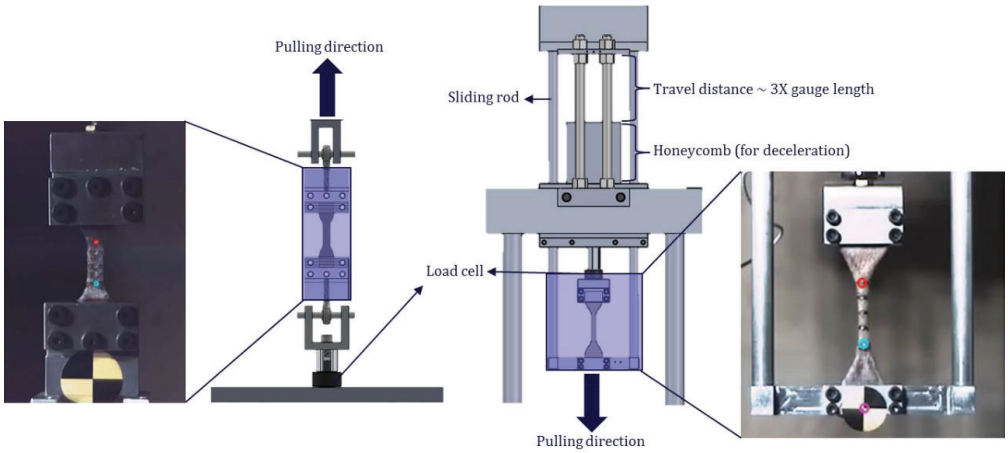

Figure 2. (left) Uniaxial static tensile test setup. A similar setup is also used for stress relaxation test. (right) Uniaxial dynamic tensile test setup. The indicated red and blue circles are video tracked to determine stretch ratio history

2.3 Stress Relaxation Tests

Stress relaxation tests were performed using the Bose ElectroForce Testing Machine (TA Instruments, New Castle, DE). The objective of these tests is to measure viscoelastic response of the tissue for implementation into constitutive models for future use in human body models. While stress relaxation tests are capable of measuring long-term viscoelastic response, the rapid step-hold process that is utilized

https://doi.org/10.52202/078352-0031

in this test type, and the methods used for processing this data, permit the measurement and identification of short-term viscoelastic responses and time-constants that are applicable to blunt impact loading. Like the uniaxial tensile test series, the dogbone samples were loaded to in-vivo length prior to testing. A displacement-controlled step-hold profile was used by subjecting the skin samples to 10%, 15%, 20%, and 30% engineering strain at the fastest loading rate (0.3m/s) achievable by the test machine without overshooting the programmed profile to obtain the instantaneous elastic response, each step was followed by a 60 seconds dwell period to collect the relaxation response. Similarly, both parallel and perpendicular samples were used for testing. The force was measured using a 50lbf (222.41N) Bose model WMC-50-456 load cell (TA Instruments, New Castle, DE) and stretch values were determined through video analysis as described in the tensile test series.

2.4 Measurements and Metrics

Engineering stress-stretch curve was constructed based on the measured force and the video tracked displacement. The engineering stress was calculated by dividing the measured force by the undeformed cross-section area. The stretch ratio was defined as the ratio between the current gauge length and original gauge length. An example of the engineering stress-stretch curve is plotted as reference (Figure 3), showing the 5 skin parameters of interest. The definition of each parameter is explained as follows:

- Ultimate tensile strength (UTS): Maximum force divided by the original cross-section gauge area.
- Strain energy: Area underneath the stress-stretch curve.
- Initial Young's modulus (E_1): Slope of the stress-stretch curve taken at the initial 5% of the UTS.
- Young's modulus (E_2): Slope of the stress-stretch curve taken in between 30% and 70% of the UTS.
- Failure stretch (λ_f): stretch ratio where the skin is completely separated.

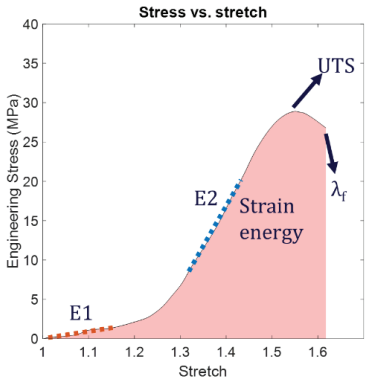

Figure 3. Typical mechanical response of human skin in tension.

Sub-failure initiates when the collagen fibers gradually break, and this was determined by investigating stiffness history (i.e. stress/stretch) of the test sample. A decrement of the stiffness after reaching the maximum indicates the sub-failure initiation and the corresponding stretch refers to the damage initiation stretch (λ^*).

2.5 Data Processing

Pre and post-test data history were recorded and a range of data of interest was determined through video analysis and force measurement data. The initial data point was determined from video analysis by tracking movement initiation of the marker within the sample gauge length. The reason to use the video analysis technique is to make sure the deformation history of the sample is captured (i.e. initial elongation with very little force) as opposed to relying on load cell information. The end data point where the failure occurred was determined when the skin sample was completely separated (i.e. no tension) is detected. The raw data was filtered using the SAE J211 standard with channel frequency class (CFC) of 600 Hz. To calculate the average response of the tensile test series where different failure stretch happened, a procedure was used where each stress-stretch curve was divided into two sections at the UTS point.

https://doi.org/10.52202/078352-0031

2.5 Statistical Analysis

A Wilcoxon Rank Sum Test (a non-parametric equivalent of two-sample t-tests) was performed using the ranksum function in MATLAB R2018b to determine the statistical significance ($p<0.05$) from the effect of strain-rate and skin orientation with respect to the Langer line on the skin response

3. RESULTS

3.1 Uniaxial Tensile Tests

The uniaxial tensile test matrix and average responses of the uniaxial tensile skin samples is summarized in Table 2. Among the 48 skin samples, 5 samples slipped out of the test fixture and were permanently deformed during testing, therefore, these samples were excluded from data analysis.

Table 2. Average uniaxial tensile test results of human skin

Orientation	Strain-rate (/s)	UTS (MPa)	Strain Energy (MPa)	E_1 (MPa)	E_2 (MPa)	λ^*	λ_f
Parallel	1 (n=11)	28.4±6.3	8.5±2.8	8.4±3.1	89.6±24.2	1.48±0.08	1.76±0.14
	75 (n=5)	20.6±7.8	7.6±3.5	10±6.5	74.2±27.3	1.36±0.10	1.75±0.18
	180 (n=6)	25.6±5.4	8.6±2.2	8.3±1.4	82.9±28.2	1.47±0.04	1.75±0.07
Perpendicular	1 (n=10)	22.6±4.6	7.1±1.2	4.2±1.0	49.5±16.5	1.74±0.12	1.97±0.15
	75 (n=5)	16.6±5.8	6±1.8	5.6±1.6	52.7±24.7	1.43±0.06	1.78±0.12
	180 (n=6)	20.7±4.9	8.5±2.4	11.0±3.3	64±21.1	1.41±0.03	1.81±0.10

For the skin samples tested at the same strain-rate, the parallel and perpendicular samples are compared and average responses for each test condition are illustrated (Figure 4). Results from the statistical analysis show the skin response to be significantly different in terms of UTS, failure stretch ($p=0.004$), initial Young's Modulus (E_1) and Young's Modulus (E_2) at the static loading rate, but no significant differences were found in both dynamic loading groups (Figure 6). The strain energy was also insignificantly different between the parallel and perpendicular samples regardless of loading rate.

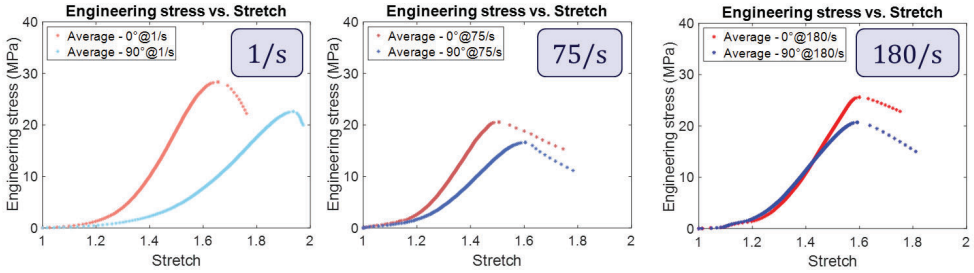

Figure 4. Comparison of skin response between different orientations under three loading rate groups

Average responses are grouped between parallel and perpendicular group to investigate the effect of strain-rate on the skin response (Figure 5). From the statistical analyses of the perpendicular samples, failure stretch ($p=0.013$) and initial Young's modulus (E_1) ($p=0.028$) were significantly different when comparing tests between 1/s and 75/s. Similar results were also observed on failure stretch and initial Young's modulus (E_1) between 1/s and 180/s loading rate group (Figure 6). However, the UTS, Young's modulus (E_2) and strain energy of the perpendicular samples were similar, and no statistical difference was found among the parallel samples between different loading rate situations.

https://doi.org/10.52202/078352-0031

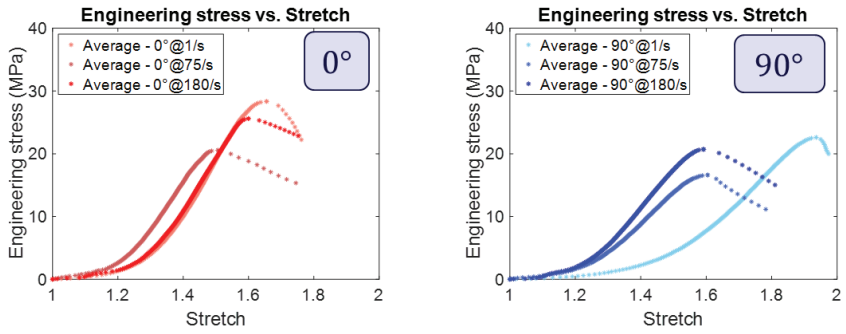

Figure 5. Comparison of skin sample response between different strain-rates at two different skin orientations (left - parallel samples, right - perpendicular samples)

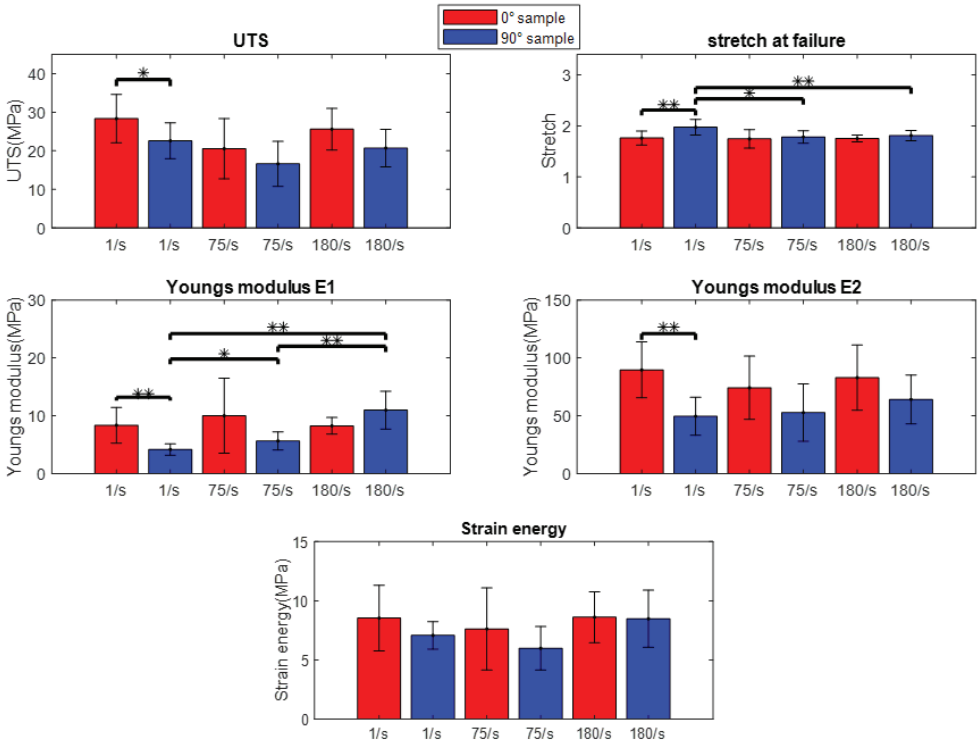

Figure 6. Wilcoxon Rank Sum Test results – 1. Effect of skin orientation with respect to Langer line on skin response under same loading rate. 2. Effect of loading rate on skin response under same skin orientation. (*p<0.05, **p<0.01)

3.2 Stress Relaxation Tests

All skin samples (n=24) were tested successfully without having slippage in the stress relaxation tests. Viscoelasticity was observed in both parallel and perpendicular samples with increasing peak stress at each ramp process followed by decaying of stress during the dwell period (Figure 7, left). Reduced relaxation function was also determined by normalizing stress decay response at each step with its corresponding peak stress. For each step-hold, the average reduced relaxation response (n=24) was calculated and an overall average reduced relaxation function (n=120) taken from all step-hold was also determined along with responses of one standard deviation (Figure 7, right).

https://doi.org/10.52202/078352-0031

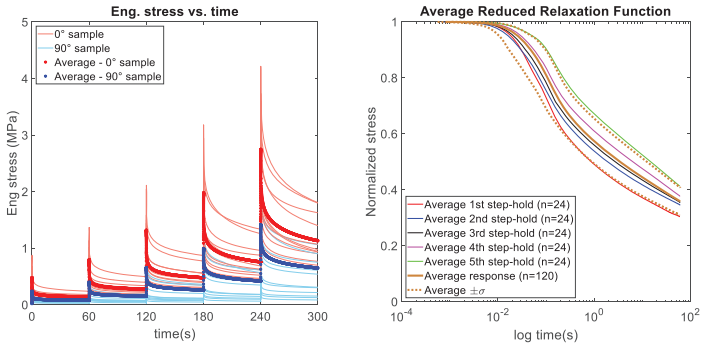

Figure 7. (left) Average stress relaxation response of parallel (thick red) and perpendicular (thick blue) skin. (right) Average reduced relaxation function of individual step-hold profile.

3.3 Sub-failure Initiation

Sub failure initiation was identified by finding maximum stiffness of the skin sample (Figure 8, left) where the stiffness was calculated at each incremental stretch value. The damage initiation stretch (λ*) of both parallel and perpendicular samples against the strain-rate is illustrated (Figure 8, right). On average, comparing the parallel and perpendicular samples, the damage initiation stretches are 1.48 vs. 1.74 in static loading group, 1.36 vs. 1.43 and 1.47 vs. 1.41 in dynamic loading groups (75/s and 180/s).

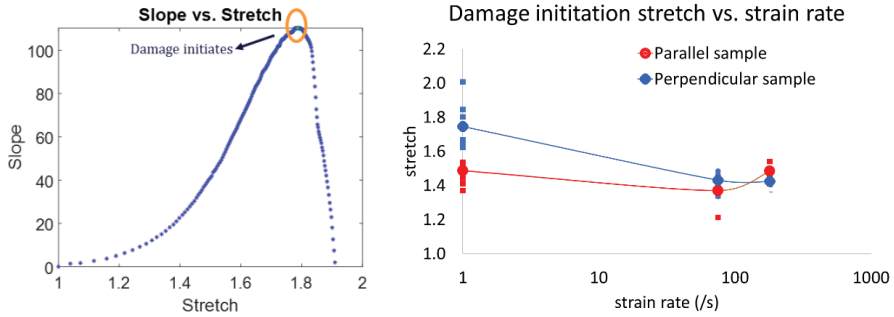

Figure 8. (left) Example of stiffness vs. stretch history of the skin sample. (right) Damage initiation stretch vs. strain-rate. Square dots are from individual samples and circular dots represent the average.

4. DISCUSSION AND CONCLUSION

4.1 Discussion

A comprehensive test matrix has been developed to fulfill the current human skin database by considering anisotropy, viscoelasticity, damage, and inter-subject variability (six human subjects) for constitutive modeling. The current study investigated skin data from a pool of a wider human population group aged between 42 and 74, producing average skin responses under different strain-rates and skin orientations. In this study, stress relaxation tests were performed to characterize skin viscoelasticity while the destructive tensile test series provide mechanical properties and damage response of the skin. To maximize the number of skin samples for the test matrix, the mechanical properties of the human back region are treated to be homogeneous, and effect of location was not considered in this study. Although skin properties have been shown to differ with body region [10], this was mainly believed due to the variation of Langer line distribution across these body regions. By characterizing two categories of skin orientation with respect to perceived Langer line, this has considered the spectrum of the skin properties at different body regions.

In the stress relaxation test, the average of the parallel skin samples exhibits higher peak stress at each step hold process when compared to the perpendicular skin samples. The peak stress on both sample types increases in a non-linear fashion as the stretch level increases. For the relaxation response, both parallel and perpendicular samples show a similar average rate of relaxation. This indicates the fiber component in the parallel sample only contributes to the instantaneous elastic response and the relaxation response is mainly dominated by the ground substance of the skin. Overall, the stress relaxation test shows the skin elastic response was non-linear and stretch independent. The results satisfy the

https://doi.org/10.52202/078352-0031

requirement of Quasi-Linear Viscoelastic (QLV) constitutive model [16] which is capable to model the temporal response of biological tissues, and this can be coupled with established hyperelastic (isotropic or anisotropic) constitutive models. The selection of the QLV model is consistent with previous efforts in the viscoelastic testing of mice skin [17].

Uniaxial tensile test data from this study were similar and within the range when compared to data from previous studies conducted on human back skin under similar loading rate conditions. However, there were differences observed on Young's modulus of the parallel and the perpendicular samples when comparing between our study and Ottenio et al. [12] at the dynamic strain-rate group (167-180/s), where we observed a lower Young's modulus. Despite having similar loading rate condition, the finding of the difference can be due to several reasons. First, the Ottenio study drew conclusions utilizing a single PMHS that was 90 years old. The elderly skins are generally believed to be stiffer and less extensible due to straightening of collagen fibers as part of the aging process [18]. Second, different testing protocol from the previous study where 2N preload was applied may have brought the skin samples to different stress state prior to testing. Unfortunately, this was the only comparable study in terms of applied strain-rate looking into the effect of loading rate and Langer line orientation on human skin. In terms of failure stretch, the definition of failure was not clearly defined across literature, hence, it was difficult to make a fair comparison of the failure stretch data. Only Ottenio et al. defined the failure as superficial tear visible on the epidermis layer. This was different from the current study as the load was still carried by the skin during superficial damage and therefore, the failure was defined as complete separation of the skin. This resulted in higher failure stretch in the current study when compared to literature.

Finally, impact velocities to the body from non-lethal blunt impacts or behind armor blunt trauma (BABT) are often an order of magnitude higher than the loading rates utilized in this study. The choice of loading conditions in this study was made based on the overarching objective of characterizing the material properties of skin for developing constitutive models that can be implemented into human body models for blunt impact simulation. Testing at higher loading rates will typically result in data with many confounding factors related to inertial effects that would limit the ability to identify the appropriate mechanical properties of the tissue. However, the loading rates tested in this study may not be a limiting factor for developing constitutive models of skin for high-rate blunt impact simulation: A) In non-lethal blunt impact and BABT, the impact occurs perpendicular to the plane of the skin and the deformation of the skin is driven by the impactor deforming into the flesh. The tensile loading rates that result from this mechanism will be lower than that of the compressive rates of the subcutaneous flesh; B) Maximum strain-rates during high-rate blunt impact only occur at an instance in time, likely during the initial impact phase where the strains are relatively low. Most of the loading and unloading of the tissue will occur at lower strain-rates, and it is likely that incorporating higher rate mechanical properties than what is currently considered will not substantially alter the overall response of the skin; and C) Our data suggests that differences in the mechanical response and failure thresholds of human skin at our highest strain-rates are relatively small and not statistically significant. This suggest that higher loading rate data will be consistent with the data collected in this study, and extrapolation of the constitutive model to higher loading rates would not result in non-biofidelic material response.

4.2 Conclusion

The current study investigated the effect of strain-rate and Langer line orientation on human skin mechanical response which produced viscoelastic and uniaxial tensile failure average curves of human skin. The following statements highlight the takeaways from this study:

- Human skin exhibits strong anisotropy behavior (UTS, E_2 and failure stretch) at static strain rate and evolves into isotropic material as strain-rate increases.
- Skin response loaded across (perpendicular) the collagen fibers are rate dependent while the response loaded along (parallel) the collagen fibers are rate independent.
- The collagen fibers within the skin are observed to be elastic with minimum viscosity due to similar relaxation response when two different skin orientations were loaded in the stress relaxation tests.
- A power trendline describing the relationship between damage initiation stretch and strain-rate is developed for the perpendicular sample. The damage initiation stretch can help to bound undamaged response of the skin where the pristine constitutive model can be applied.
- The data generated in this study is likely applicable to non-lethal blunt impacts and behind armor blunt trauma (BABT), with the caveat that the strain-rates tested in this study may not encompass the entire loading history of these types of impact events.

https://doi.org/10.52202/078352-0031

With the experimental curves presented in this study, the test curves can be converted into true stress-stretch response before developing a constitutive model to capture dynamic tensile test response of human skin. Ultimately, this data will be used to develop constitutive models of skin for use in simulating blunt impact events with human body models, and will be beneficial for developing a biofidelic, physical skin simulants for the future testing and evaluation of blunt impactor performance.

Acknowledgments

This study was supported by the U.S. Army Aberdeen Test Center under Contract No W91CRB-17-C-0032.

References

[1] Jones, R. E., Foster, D. S., and Longaker, M. T. (2018). Management of Chronic Wounds—2018. JAMA, 320(14), 1481–1482.
[2] Haut, R. C. (1989). The Effects of Orientation and Location on the Strength of Dorsal Rat Skin in High and Low Speed Tensile Failure Experiments. Journal of Biomechanical Engineering, 111(2), 136–140.
[3] Arumugam, V., Naresh, M. D., and Sanjeevi, R. (1994). Effect of strain rate on the fracture behaviour of skin. Journal of Biosciences, 19(3), 307–313
[4] Pramudita, Jonas A., Shimizu, Y., Tanabe, Y., Ito, M. and Watanabe, R. (2014). Tensile Properties of Porcine Skin in Dorsal and Ventral Regions. Journal of JSEM, Vol.14, Special Issue (2014) s245-s250.
[5] Papy, A., Robbe, C., Nsiampa, N., Oukara, A., and Goffin, J. (2012). Definition of a standardized skin penetration surrogate for blunt impacts. IRCOBI Conference 2012.
[6] Bir, C. A., Resslar, M., & Stewart, S. (2012). Skin penetration surrogate for the evaluation of less lethal kinetic energy munitions. Forensic Science International, 220(1–3), 126–129.
[7] Pramudita, Jonas A., Sasaki, M., Ito, M., Watanabe, R. and Tanabe, Y. (2016). Mechanical Characterization of Soft Tissue Simulant Materials. Advanced Experimental Mechanics, Vol.2, (2017), 135-140.
[8] Joodaki, H., and Panzer, M. B. (2018). Skin mechanical properties and modeling: A review. Proceedings of the Institution of Mechanical Engineers, Part H: Journal of Engineering in Medicine, 232(4), 323–343.
[9] Jacquemoud, C., Bruyere-Garnier, K., and Coret, M. (2007). Methodology to determine failure characteristics of planar soft tissues using a dynamic tensile test. Journal of Biomechanics, 40(2), 468–475
[10] Ní Annaidh, A., Bruyère, K., Destrade, M., Gilchrist, M. D., and Otténio, M. (2012). Characterization of the anisotropic mechanical properties of excised human skin. Journal of the Mechanical Behavior of Biomedical Materials, 5(1), 139–148.
[11] Gallagher, A.J., Ní Annaidh, A., Bruyere, K., Otténio, M., Xie, H., and Gilchrist, M.D. (2012). Dynamic Tensile Properties of Human Skin. IRCOBI Conference 2012.
[12] Ottenio, M., Tran, D., Ní Annaidh, A., Gilchrist, M.D., and Bruyère, K. (2015). Strain rate and anisotropy effects on the tensile failure characteristics of human skin. Journal of the Mechanical Behavior of Biomedical Materials, 4(1), 241-250.
[13] Khatyr, F., Imberdis, C., Vescovo, P., Varchon, D., and Lagarde, J.-M. (2004). Model of the viscoelastic behaviour of skin in vivo and study of anisotropy. Skin Research and Technology, 10(2), 96–103.
[14] Piérard, G. E., Piérard, S., Delvenne, P., and Piérard-Franchimont, C. (2013). In Vivo Evaluation of the Skin Tensile Strength by the Suction Method: Pilot Study Coping with Hysteresis and Creep Extension. ISRN Dermatology, 2013, 1–7.
[15] Langer, K., 1978. On the anatomy and physiology of the skin—I. The cleavability of cutis. Br. J. Plast. Surg. 31, 3–8.
[16] Fung, Y.-C. (1993). Biomechanics: Mechanical Properties of Living Tissues. New York: Springer-Verlag. p. 568. ISBN 0-387-97947-6.
[17] Wang, Y., Marshall, K. L., Baba, Y., Lumpkin, E. A., and Gerling, G. J. (2015). Compressive Viscoelasticity of Freshly Excised Mouse Skin Is Dependent on Specimen Thickness, Strain Level and Rate. PLOS ONE, 10(3), e0120897.
[18] Tonge, Theresa K., Atlan, Lorre S., Voo, Liming M., and Nguyen, Thao D. (2019). Full-field bulge test for planar anisotropic tissues: Part I – Experimental methods applied to human skin tissue. Acta Biomaterialia, 9(2013) 5913-5925.

https://doi.org/10.52202/078352-0031